Chapter

Nanomanipulation with Designer Thermoplasmonic Metasurface

Chuchuan Hong, Sen Yang and Justus Chukwunonso Ndukaife

Abstract

Plasmonic nanoantennas provide an efficient platform to confine electromagnetic energy to the deeply subwavelength scales. The resonant absorption of light by the plasmonic nanoantennas provides the means to engineer heat distribution at the micro and nanoscales. We present thermoplasmonic metasurfaces for on-chip trapping, dynamic manipulation and sensing of micro and nanoscale objects. This ability to rapidly concentrate objects on the surface of the metasurface holds promise to overcome the diffusion limit in surface-based optical biosensors. This platform could be applied for the trapping and label-free sensing of viruses, biological cells and extracellular vesicles such as exosomes.

Keywords: metasurface, nano-antenna, thermoplasmonic, optofluidic, nano-tweezer

1. Introduction

As an important category of metamaterials [1–4], which are artificial structures designed to achieve unique properties not occurring in nature, electromagnetic metasurfaces are able to provide unique electromagnetic responses for complete control over the phase, amplitude or polarization of light in a two-dimensional platform [5–9]. There are numerous kinds of applications that can be enabled by metasurfaces including holograms, metalens, near-eye displays, vortex beam generators and compact Spatial Light Modulators (SLM) [9–12] (**Figure 1**).

A meta-atom is the building block of a metasurface and it is usually a resonator made of either plasmonic or dielectric materials. In this section, we will focus on plasmonic metasurfaces to emphasize the significance of plasmonic metasurfaces for diverse applications, including on-chip optical trapping and optofluidic control. We will also present thermoplasmonic metasurfaces capable of inducing microfluidic motion in microchannels based on electrothermoplasmonic (ETP) effect, and discuss their role in on-chip nanoparticle trapping and manipulation [16–19].

Noble metals such as gold (Au) or silver (Ag) are typically used as plasmonic materials at visible or near-IR frequencies. Due to their ability to sustain plasmon oscillation, a well-designed metallic nanostructure can confine light in a very tiny volume, which generally creates a smaller mode volume than dielectric structures, especially at the resonance frequency. Hence, plasmonic resonators can tightly confine light in a tiny region so that they largely enhance the local electric field intensity. Furthermore, due to the Ohmic losses, the plasmonic materials generate heat under illumination. The enhanced local electric field results in efficient local

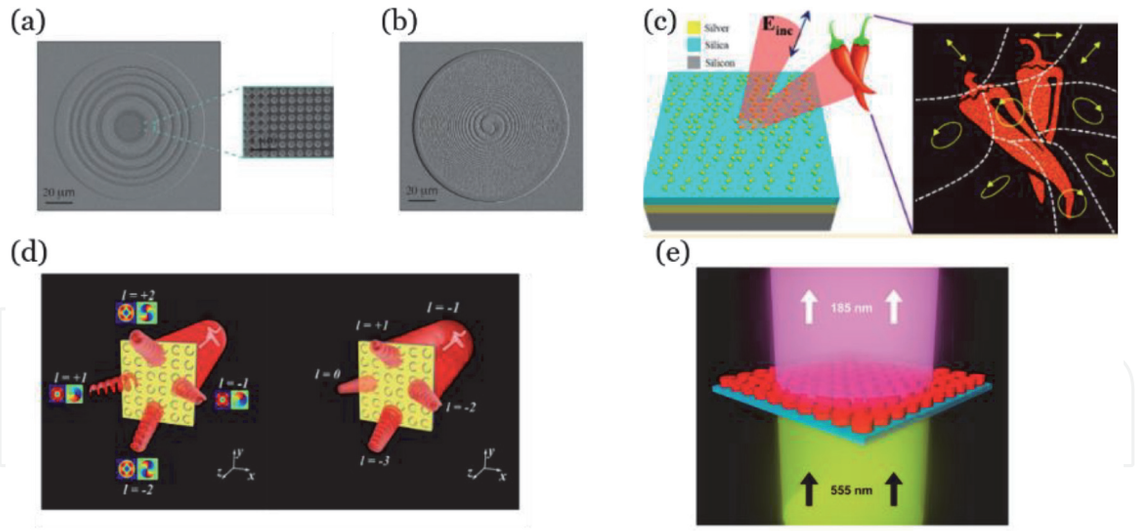

Figure 1.
Various applications based on metasurfaces. (a) SEM image of metasurface lens composed of silicon nano-post array. (b) SEM image of a vortex beam generator made of silicon nano-post array. (c) A plasmonic metasurface hologram insensitive to light polarization states. (d) A vortex beam opto-multiplexer and demultiplexer made of gold at terahertz. (e) A titanium dioxide metasurface enhancing third harmonic generation to produce ultraviolet light. Images: (a) and (b) are adapted from [9] Copyright © 2016 American Chemical Society, (c): [13] Copyright © 2018 American Chemical Society, (d) [14] Copyright © 2017 American Chemical Society and (e) [15] Copyright © 2019 American Chemical Society.

heating. Although, several research works in the literature have considered the loss in plasmonics as detrimental, it is now known that the loss in plasmonics can be beneficial to fast on-chip nano-particle manipulation [17, 20]. The loss-induced heating effect has given rise to the burgeoning field of thermoplasmonic metasurface.

2. Optical trapping and optical tweezers

Optical tweezer, which employs a tightly focused laser to trap microscopic objects have proven to be a versatile tool for many scientific researches such as in biophysics [21] and was recently recognized with a 2018 Physics Nobel prize. The initial experiment to trap particles with a laser beam used two counter-propagating loosely focused beams to localize the particles at a node of the generated standing wave, and this was reported by Arthur Ashkin and his colleagues in 1970 [22]. Subsequently, a single beam optical tweezer, which employs a tightly focused laser beam to achieve three-dimensional manipulation and trapping of microscale particles was demonstrated in 1986 [23]. Dielectric particles are trapped when the refractive index of the particles is higher than the refractive index of the surrounding medium.

Generally, the optical force is decomposed into two parts, the gradient force and the scattering force. The scattering force is also called radiation pressure and acts in the direction of light propagation. The gradient force is the significant part in single beam optical trapping procedure, because it is oriented perpendicular to the axis and push particles towards a region with higher optical intensity. Thus, the gradient force ensures that a particle is trapped in an optical tweezer. The total optical force induced on a particle can be determined by Maxwell's Stress Tensor method (MST). When the size of the particle is much smaller than the wavelength of trapping light, the particle can be considered as a dipole, so that the dipole approximation can be

applied to simplifying the calculation of the optical force [24]. The detailed derivation of MST and dipole approximation can be obtained in Ref. [25].

In biological applications, target particles range in size from micrometer size scales such as cells and nanometer length scales such as viruses, protein molecules and vesicles. Trapping nanoscale particles is challenging in free-space optical tweezers. There are two main challenges faced by researchers using optical tweezers. The first challenge arises because the value of the gradient force is proportional to the third power of the radius of the particles in the quasi-static limit. Secondly, the optical gradient force is proportional to the gradient of light field intensity, and it is thus limited because the diffraction limit limits the achievable gradient in the light field intensity. One approach explored by Ashkin to increase the trapping stability for nanoscale objects in free-space optical tweezers involves the use of very high optical powers. However, this results in serious damage to the objects being trapped, a process termed opticution.

3. Plasmonic optical tweezers

In order to overcome the limit on particle size that can be trapped in conventional optical tweezers, plasmonic optical tweezers have been proposed Novotny et al. [17, 26–33]. Plasmonic optical tweezers employ plasmonic nanoantenna, which can squeeze light to nanoscale volumes comparable to the size of the target particles, thus significantly enhancing the gradient force applied on nanoscale particles. Unlike the light-matter interaction between dielectric materials and electromagnetic wave, plasmonic materials uniquely react to the light field through free-electron-photon coupling to generate a specific type of surface wave called surface plasmon polariton (SPP). Furthermore, a subwavelength plasmonic particle will efficiently couple to propagating light to generate localized surface plasmon resonance (LSPR) and further enhance the electric field due to this resonance. These phenomena permit light to be strongly localized at deep subwavelength scales. Besides, surface plasmon structures offer additional advantages on lab-on-a-chip manipulation due to its compatibility with integrated photonics devices [34, 35].

There are two main challenges with the use of plasmonic nanoantennas for near-field nano-optical tweezers. These challenges include the Ohmic loss in the materials, which invariably results in loss-induced heating, and the need to rely on slow Brownian diffusion to transport particles towards the illuminated nanoantenna. The Ohmic loss in plasmonic materials at visible or near-IR is inevitable. It will not only hamper the efficiency of particle trapping due to the need to generate enough trapping potential energy to overcome the Brownian motion and possible thermophoretic force, but the heat generated by Ohmic loss would be problematic in many experiments. Though the light field is tightly confined near an illuminated plasmonic nanoantenna leading to very high field intensity enhancement [16], which are advantageous for particle trapping, the damage from temperature rise due to this field enhancement affects the experimental trapping stability in several ways. Experimentally, bioparticles are vulnerable in an environment with increasing temperature. Furthermore, excessive photothermal heating could deform the plasmonic nanoantenna [36]. In aqueous solutions, this heating effect would even generate bubbles by boiling the water and disrupt the entire experiment. Wang et al. demonstrated that by integrating a heat sink in plasmonic tweezers made up of layers of high thermal conductivity materials, the adverse effects arising from the heating effect can be mitigated [37].

Rather than treating the photothermal heating effect as detrimental in plasmonic nanotweezer experiments, plasmonic heating can be harnessed to enable new

functionalities in near-field nano-optical trapping. Ndukaife et al. proposed and demonstrated that thermal effect due heating loss can actually promote the trapping process thereby eliminating the need to rely on slow Brownian diffusion to deliver particles towards the plasmonic nanotweezer [18, 20]. This new platform, referred to as electrothermoplasmonic tweezers harnesses the localized photothermal heating from an illuminated plasmonic nanoantenna to establish a thermal gradient in the fluid. The thermal gradient results in a gradient in the permittivity and electrical conductivity of the fluid. An applied AC electrical field acts on these gradients to result in rapid microfluidic flow motion, which transports particles towards the plasmonic hotspot. This typical fluid motion is called electrothermoplasmonic (ETP) flow. Under this condition, heating effect actually speeds up the loading procedure and converts the slow traditional diffusion-based particle loading of conventional plasmonic nano-tweezers into a fast and directional particle loading in electrothermoplasmonic tweezers. The technique works with small temperature rises of a few degrees and only the thermal gradient needs to be optimized, thereby making it suitable for handling biological objects.

By all means, plasmonic optical tweezers are promising and especially useful for manipulation of extremely small particles. By careful thermal engineering to mitigate excessive heating effect, plasmonic optical tweezers can be utilized to enable many applications.

4. Electrothermoplasmonic, electro-osmotic and thermophoretic effects

As mentioned in the previous section, the heating effect from plasmonic nanoantennas can be utilized to enable new capabilities in near-field nano-optical trapping. The physics nature behind this kind of trapping comprises the interplay of multiple physical phenomena. In this section, we describe several forces that can be experienced by objects in electrothermoplasmonic tweezers in the presence of optical illumination and applied AC electric field. To understand how the thermal effect influences the trapping process, we firstly look at the thermophoresis phenomenon, which is the motion of particles or molecules in the presence of thermal gradients. Unlike the normal diffusion process due to Brownian motion, thermophoresis is induced by a temperature gradient ∇T to cause the drifting of particles. In most cases, particles prefer to move towards the region of lower temperature, away from the plasmonic nanoantenna. This trend is called "thermophobic" behavior or positive thermophoresis. However, this motion can be reversed in certain instances whereby particles will move towards the region of higher temperature, which is called "thermophilic" behavior, also known as negative thermophoresis.

Quantitatively, in a diluted suspension (particle weight fraction w $<<$ 1), the mass flow J can be written as [38, 39]:

$$J \approx -D\nabla c - cD_T\nabla T, \tag{1}$$

where D and D_T are the Brownian diffusion coefficient and thermodiffusion coefficient, respectively.c denotes the concentration. In diluted concentrations, thermodiffusion velocity is generally assumed to be linearly dependent on the temperature gradient ∇T with the thermodiffusion coefficient D_T:

$$\vec{v} = -D_T\nabla T \tag{2}$$

Under steady-state, the thermodiffusion is balanced by ordinary diffusion and the concentration coefficients are related in an exponential law:

$$c/c_0 = \exp\left[-(D_T/D)(T - T_0)\right] \tag{3}$$

Finally, the thermophoretic force induced by thermal gradients on a particle in the fluid is given by [40]:

$$F_{therm} = -K_b T(z) S_T \nabla T \tag{4}$$

Here, K_b stands for Boltzmann's constant and $T(z)$ corresponds to the temperature at a given position z. Soret coefficient S_T is defined as the ratio: $S_T = D_T/D$, which depicts how strong the thermodiffusion is at steady state. The Soret coefficient is influenced by many factors including temperature, size of the particles, surface charge of the particles and ions in the solvent. From Eq. (4), we concluded that the thermophoretic force is proportional to Soret coefficient but with opposite sign. It is useful to know that Soret coefficient is also temperature dependent and flips its sign from positive to negative by decreasing temperature, as expressed in Eq. (5) [38, 39]. S_T^{∞} represents a high-T thermophobic limit and T^* is the temperature where S_T switches sign, and T^0 embodies the strength of temperature effects. At that moment, force applied onto particles switches its orientation from "thermophobic" to "thermophilic" behavior.

$$S_T(T) = S_T^{\infty}\left[1 - \exp\left(\frac{T^* - T}{T^0}\right)\right] \tag{5}$$

The direction of the thermophoretic force can be tuned from a repulsive to an attractive force by tuning the interfacial permittivity of the electrical double layer (EDL) surrounding the particles in solution. The EDL exists on the surface of an object when it is exposed to a fluid. The object could be a small charged particle floating inside the liquid or a surface coated with fluid. The charged object attracts counterions from the solution to screen the surface charge. This layer is called the Stern layer. This charged object consequently attracts ions from the liquid with opposite charge via Coulombic force to electrically screen the first layer and the particle. The second layer is called diffuse layer. The potential difference across the diffuse layer is defined as Zeta potential, ζ. The charges in the diffuse layer are not as tightly anchored to the particle as the first layer and the thickness can be affected by tangential stress [41].

Based on Anderson's model [42], the thermophoretic mobility of the particle is associated with its Zeta potential.

$$D_T = -\frac{\varepsilon}{2\eta T}\frac{2\Lambda_1}{2\Lambda_1 + \Lambda_p}\left(1 + \frac{\partial ln\varepsilon}{\partial lnT}\right)\zeta^2 \tag{6}$$

where ε is the solvent permittivity, and Λ_1 and Λ_p are the thermal conductivities of the solvent and the particle, respectively. In bulk water, for example, the differential permittivity change with temperature $\frac{\partial ln\varepsilon}{\partial lnT} = -1.4$ at room temperature. In building up the model of ET flow numerical analysis, this term can be taken into account to ensure the accuracy of the results [16]. Inside an EDL, however, the value of $\frac{\partial ln\varepsilon}{\partial lnT}$ can reach +2.4, which is crucial to reverse the Soret coefficient and induce a negative thermophoresis behavior. Hence, one way to induce negative thermophoresis behavior is to ensure that an EDL has been established, by charging the surface of the particles. Adding surfactants, such as Cetyltrimethylammonium Chloride (CTAC), for example, into particle solution can help to build up an EDL on the particles [27].

The photothermal heating of the fluid by the plasmonic nanoantennas can also be utilized to induce strong electro-convection fluidic motion, which is called electrothermal (ET) effect. When the temperature inside fluid is no longer uniform due to a thermal gradient, a gradient in the permittivity and the conductivity of the fluid will induced as well. In such a system, a local free charge distribution must be present if Gauss's Law and charge conservation are to be satisfied simultaneously. When an AC electric field is applied, both free and bounded local charge density responds to the applied electric field so that a non-zero body force is generated on the fluid:

$$f_{ET} = \rho_e E - \frac{1}{2}|E|^2 \nabla \varepsilon_m \tag{7}$$

After perturbative expansion in the limit of small temperature gradient, the force density is expressed as [43]:

$$f_{ET} = \frac{1}{2} Re\left\{\frac{\varepsilon(\alpha-\beta)(\nabla T.E)E^*}{\sigma + i\omega\varepsilon} + \frac{1}{2}\varepsilon\alpha|E|^2\nabla T\right\} \tag{8}$$

where $\alpha = {}^1\!/_{\varepsilon}\frac{d\varepsilon}{dT}$ and $\beta = {}^1\!/_{\sigma}\frac{d\sigma}{dT}$. ε stands for permittivity and σ stands for conductivity. ω is the AC frequency. So far, the body force is decomposed into two parts: the first term on the right-hand side of Eq. (7) is the Coulombic force, and it increases as AC frequency goes down. It is worth mentioning that this electrothermal flow is able to generate a fast flow to rapidly transport particles from a long distance of several hundreds of microns to the hot spot. One no longer need to wait for particles to diffuse through Brownian motion into the target region to be successfully trapped.

Based on this concept, a novel plasmonic nano-tweezer called electrothermoplasmonic tweezers using a single plasmonic nanoantenna was invented [18, 44]. In this platform, a plasmonic nanoantenna is illuminated causing the surrounding fluid near the nanoantenna to be slightly heated up due to the Ohmic loss nature of plasmonic materials. Localized heating of fluid medium induces local gradients in the fluid's electrical conductivity and permittivity. An applied AC electric field acts on these gradients to induce an electrothermal microfluidic flow, which acts to transport particles towards the illuminated plasmonic nanoantenna.

The electrothermal flow from plasmon-induced heating can be modeled through the solution of the electromagnetic wave-equation, heat equation and the Navier-Stokes equation. Mathematically, we can solve the wave equation to find the electric field in the vicinity of the plasmonic nanoantenna:

$$\nabla \times (\nabla \times E) - k_0^2 \epsilon(\mathbf{r})\mathbf{E} = 0 \tag{9}$$

The heat source density generated by plasmonic heating is calculated using the electric field distribution and the induced current density representing the energy loss:

$$\mathrm{q(r)} = \frac{1}{2} Re\,(\mathrm{J}\cdot\mathbf{E}^*) \tag{10}$$

The temperature field distribution is determined by solving the heat equation below:

$$\nabla\cdot[-\kappa\nabla\mathrm{T}(\mathbf{r}) + \rho c_P \mathrm{T}(\mathbf{r})\mathrm{u}(\mathbf{r})] = q(\mathbf{r}) \tag{11}$$

Finally, the Navier-Stokes equation is solved to find the velocity of the fluid:

$$\rho_0[\mathrm{u}(\mathbf{r}) \cdot \nabla]\mathrm{u}(\mathbf{r}) + \nabla p(\mathbf{r}) - \eta\nabla^2\mathrm{u}(\mathbf{r}) = \mathbf{F}, \tag{12}$$

where **F** here is the electrothermal force described in the prior section [43]. We have also established the theoretical framework between the ETP flow velocity with laser power and external AC electric field. It is noted that the ETP flow velocity scales linearly with laser power and quadratically with AC electric field amplitude [16].

Electro-osmotic flow is another category of body flow happening in a microfluidic channel [45]. Electro-osmosis occurs when tangential electric field acts on the loosely bound charges in the EDL along the channel walls. Because of the existence of electrical double layer, near the charged channel walls the tangential electric field will act on the EDL charges to induce an electro-osmotic flow with slip velocity given by:

$$\mathrm{u_s} = -\frac{\varepsilon_\mathrm{w}\zeta}{\eta}\mathrm{E}_\parallel \tag{13}$$

where $\mathrm{E}_\parallel$ is the tangential component of the bulk electric field, η is the fluid viscosity and ζ is the zeta potential. When there is a plasmonic structure existing inside a microfluid channel on the channel wall, this plasmonic structure perturbs the AC electric field, resulting in a non-zero tangential component of the AC electric field. For instance, Jamshidi or Hwang and their colleagues integrated photoconductive material as the electrode of applied bias inside a microfluidic channel to design a so-called "NanoPen" device for dynamical manipulation on particles using low-power laser illumination [46, 47].

This perturbed external electric field not only contributes to electro-osmosis, but could also induce a dielectrophoretic force on the suspended particles [48]. Particles experience dielectrophoresis only when the external field is non-uniform and the force that particles feel, the DEP force, does not depend on the polarity of the AC field. DEP can be observed both in AC or DC electric field. There is a crucial evaluator for DEP force direction called Clausius-Mossoti factor.

$$\mathrm{K} = \frac{\varepsilon_2 - \varepsilon_1}{\varepsilon_2 + 2\varepsilon_1} \tag{14}$$

In terms of Clausius-Mossoti factor, the DEP force is expressed as:

$$\mathrm{F_{DEP}} = 2\pi\varepsilon_1 R^3 K \nabla E_0^2 \tag{15}$$

From which, we understand DEP force is proportional to particle volume and magnitude of K. The direction of DEP force is along the gradient of the electric field intensity and its sign depends on the sign of Clausius-Mossoti factor.

In AC field and lossy medium, the Clausius-Mossoti factor is frequency dependent and it is given by:

$$\mathrm{K} = \frac{\varepsilon_2^* - \varepsilon_1^*}{\varepsilon_2^* + 2\varepsilon_1^*}, \varepsilon_1^* = \varepsilon_1 + \frac{\sigma_1}{j\omega} \text{ and } \varepsilon_2^* = \varepsilon_2 + \frac{\sigma_2}{j\omega} \tag{16}$$

The Clausius-Mossoti factor determines whether the DEP force is attractive or repulsive ant it depends on the frequency of AC field and electric properties of particles and medium.

So far, we have briefly introduced the main mechanisms which could occur in plasmonic nanotweezers. The physical phenomena could be harnessed to introduce new capabilities in plasmonic nanotweezers. A recent article [49] has proposed the use of DEP force to promote particle transport towards plasmonic resonators.

5. Thermoplasmonic nanohole metasurface

In this section, we discuss thermoplasmonic nanotweezer based on nanohole metasurface [50], which enables high-throughput large-ensemble nanoparticle assembly in a lab-on-a-chip platform. As mentioned in previous sections, optical metasurfaces achieve control over the properties of light. Besides the optical response, thermoplasmonic metasurfaces allow to engineer the thermal response at micro and nanoscale. Upon illumination of metasurface, the combination of optical and thermal effects enables robust large-ensemble many-particle trapping.

The nanohole metasurface comprises of an array of subwavelength nanoholes in a 125 nm thick gold film and illuminated with a laser of 1064 nm wavelength. This nanohole metasurface serves as a plasmonic resonator supporting both the localized surface plasmon resonance (LSPR) and Bloch mode surface plasmon polariton (SPP). Due to the plasmon response, electromagnetic field is confined near the rims of the nanohole and the region in between nanohole, as depicted in **Figure 2**. This enhances the photothermal conversion efficiency and hence higher temperature rise under illumination of the structured plasmonic film. As predicted, when an external AC field is applied onto the nanohole metasurface, a long-range electrothermo-plasmonic (ETP) flow is generated inside the fluid, bringing particles from long distance towards the hot spot. Simultaneously, because of the existence of nanohole array, the AC electric field in the channel is no longer uniform but tangential components are created, which induces AC electroosmotic flow. The numerical simulation results of electroosmotic flow are depicted in the **Figure 3**.

For the experimental demonstration, the gold metasurface is fabricated using template stripping method on a silicon wafer. Using standard nanofabrication procedures, an array of nanoholes are fabricated on a silicon wafer, which is the same dimension and scale as the nanohole array on gold film. A 125 nm gold film is then deposited onto this silicon template using an electron beam evaporation process. Finally, a UV-sensitive curing-agent was uniformly spread onto the gold film and covered by an ITO-coated glass substrate with the same size as the silicon template.

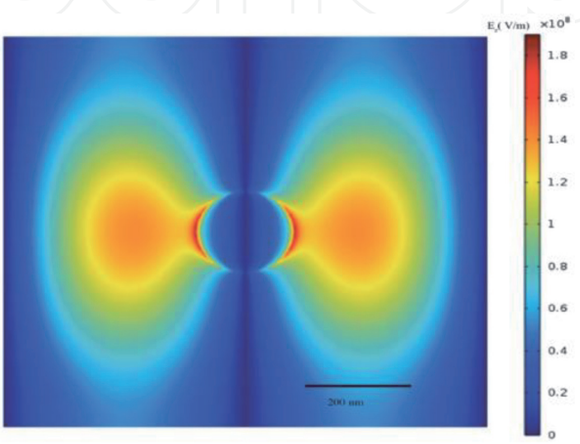

Figure 2.
Electric field distribution of one of the single nanoholes by numerical simulation. Adapted with permission from Ref. [50]. Copyright (2018) American Chemical Society.

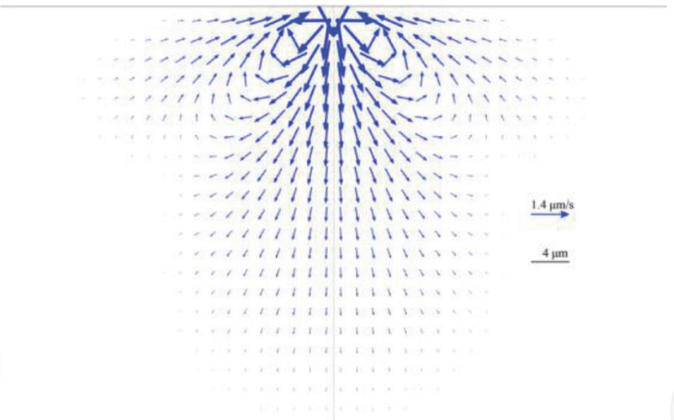

Figure 3.
Velocity profile of the induced AC electro-osmosis flow from numerical simulation. Adapted with permission from Ref. [50]. Copyright (2018) American Chemical Society.

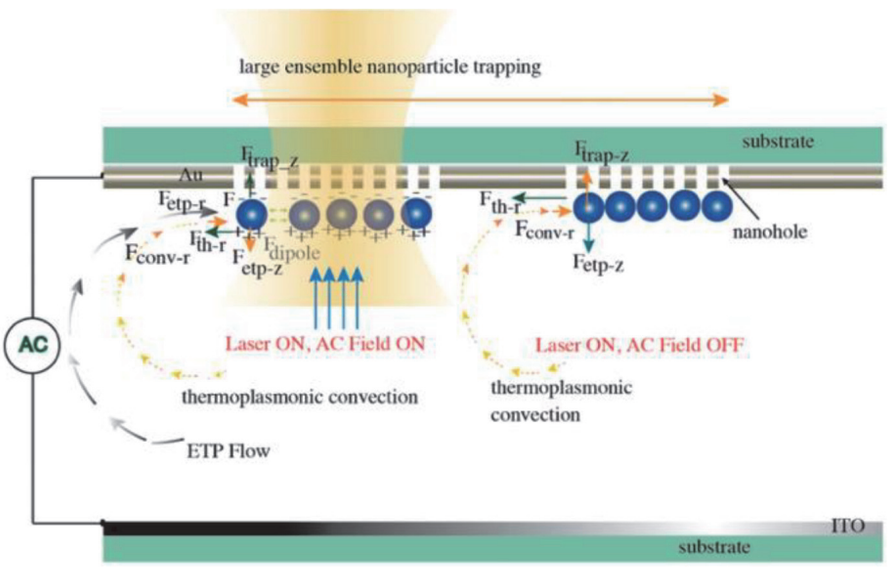

Figure 4.
Illustration of microfluidic chip coupling with nanohole plasmonic metasurface. Adapted with permission from Ref. [50]. Copyright (2018) American Chemical Society.

After UV illumination is applied to harden the curing-agent, the gold film layer is stripped off and transferred to a glass substrate by gently inserting a blade in between the gold film and silicon template due to the weak attachment between gold and silicon. The silicon template can be cleaned by soaking in hydrogen peroxide and sulfuric acid solution in the ratio 3:1 to remove the organics on the surface and any remaining gold flakes on the template. Furthermore, the residual gold remaining on the template can be removed thoroughly by a gold etchant. The template can be reused multiple times.

To make the gold nanohole metasurface into a microfluidic chip, another ITO-coated glass coverslip is placed above the nanohole array sample, with a 120 μm dielectric spacer in between. For the trapping experiments, a dilute solution of 1 μm PS beads was injected into the channel. AC electric field is applied in between the ITO-coated glass cover slip and gold film. A 1064 nm laser illumination is focused on the nanohole array. The mechanism of particle trapping in the thermoplasmonic nanohole metasurface channel is depicted in **Figure 4**. The strong photo-induced heating in combination with an applied AC electric field creates the ETP flow that enables long-range capture and transport of particles towards the laser position. The

particles brought close to the nanohole array are trapped by the optical gradient force. In the lateral direction, the particle-particle separation distance is tuned by the dipole-dipole repulsion force between the particles [51, 52].

Under the microscope, when both laser illumination and AC electric field is turned on, particles are seen moving very directionally towards the nanohole metasurface. By selectively turning on and off AC electric field, particle-particle spacing can be controlled dynamically, due to the polarization of the particles induced by AC electric field. Briefly, particles are polarized by the AC field and a dipole-dipole repulsive force creates an in-plane interparticle separation between them. The ETP flow is measured experimentally using microparticle image velocimetry and its radial velocity is shown in **Figure 5(a)**.

Experimental images of trapped particles on the surface of the nanohole array are depicted in **Figure 5(b)**. When both the laser illumination and the AC electric field are applied, the particles are trapped with a certain interparticle spacing between them due to the in-plane dipole-dipole repulsion force. When the AC field is turned off, with the laser still on, the AC electric field-induced dipole-dipole repulsion force disappears, and the assembly becomes more compact.

They also show that the ETP flow induced by the array of nanohole is higher than that can be achieved with a single nanohole or an unpatterned gold film. The plasmonic resonance induced by patterned nanohole truly enhances the electro-thermal effect. These results obtained from micro-particle image velocimetry analysis are depicted in **Figure 6**.

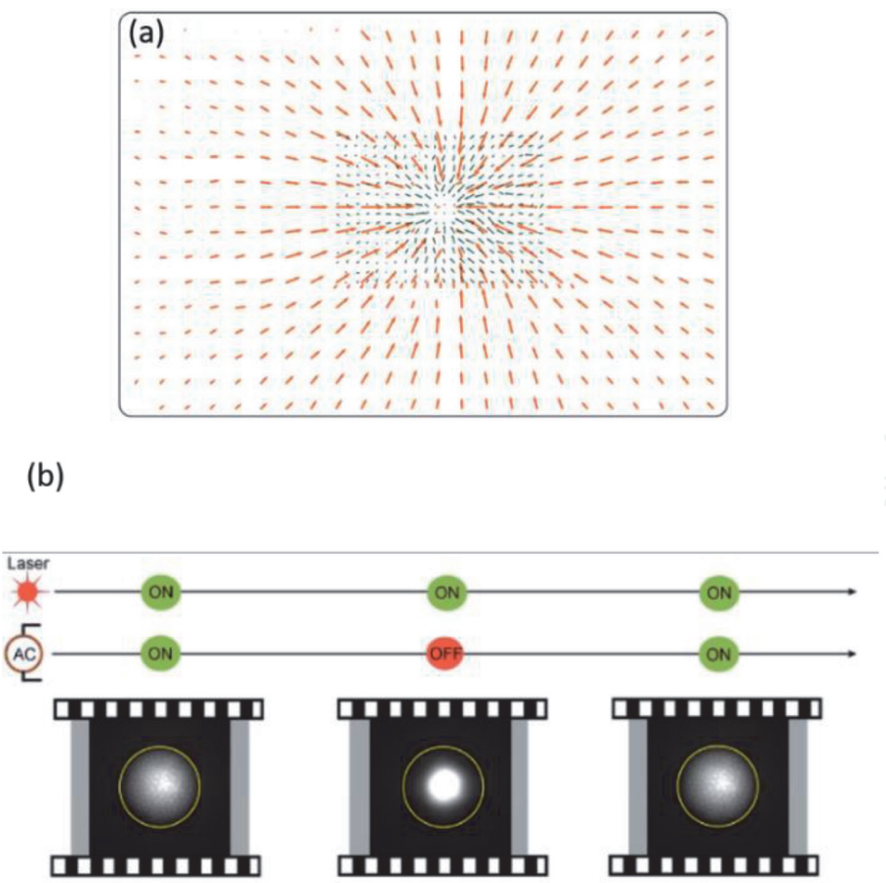

Figure 5.
(a) Experimentally measured radial velocity of the ETP flow (b) sequence of trapping and particle assembling of 200 nm diameter polystyrene beads on the surface of the plasmonic nanohole array when AC field is alternatively turned on and off. Adapted with permission from Ref. [50]. Copyright (2018) American Chemical Society.

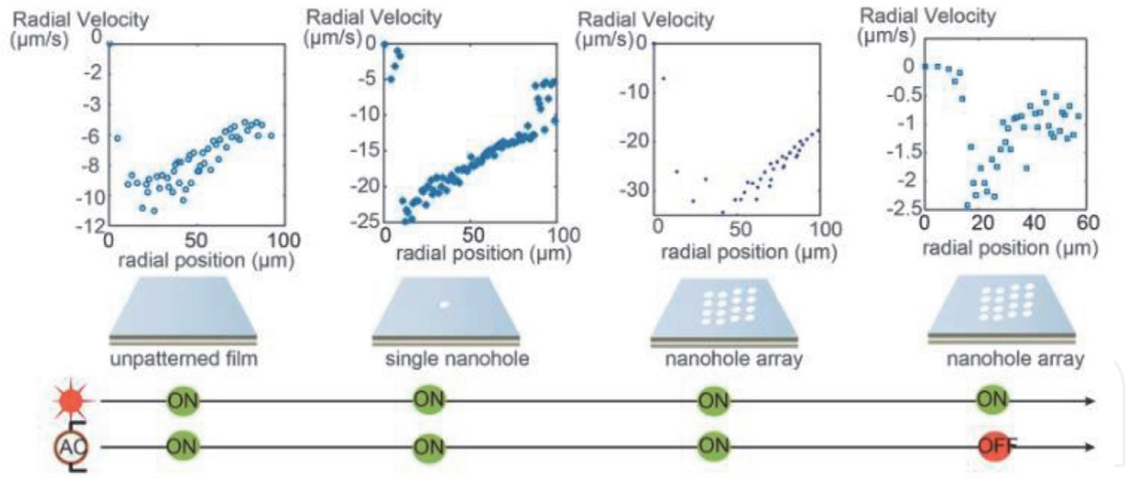

Figure 6.
The nanohole array enables an enhanced ETP flow that is higher than the velocity induced when the planer film or a single nanohole is excited. Adapted with permission from Ref. [50]. Copyright (2018) American Chemical Society.

6. Conclusion

We have introduced the importance of plasmonic metasurface for applications in optical trapping, nano-tweezers and tiny particle manipulation, by demonstrating a nanoparticle trapping approach that utilizes a thermoplasmonic nanohole metasurface. The application of laser illumination and a.c. electric field results in new physical effects such as electrothermoplasmonic flow and a.c. electroosmosis that can work in concert with optical gradient forces to enable to new advanced features in micro and nanoparticle manipulation. The recent reports in the literature as articulated in this section shows that the intrinsic loss in plasmonic systems is not always detrimental but could work in synergy with the high electric field enhancement to realize advanced lab-on-a-chip devices in nanomanufacturing, nanophotonics, life science and quantum optics.

Acknowledgements

The authors acknowledge support from NSF ECCS-1933109 and Vanderbilt University.

Conflict of interest

The authors declare no conflict of interest in this book section.

Author details

Chuchuan Hong[1,2], Sen Yang[2,3] and Justus Chukwunonso Ndukaife[1,2]*

1 Department of Electrical Engineering and Computer Science, Vanderbilt University, Nashville, TN, USA

2 Vanderbilt Institute of Nanoscale Science and Engineering, Vanderbilt University, Nashville, TN, USA

3 Interdisciplinary Materials Science, Vanderbilt University, TN, USA

*Address all correspondence to: justus.ndukaife@vanderbilt.edu

References

[1] Liu Y, Zhang X. Metamaterials: A new frontier of science and technology. Chemical Society Reviews. 2011;**40**(5): 2494

[2] Smith DR. Metamaterials and negative refractive index. Science. 2004;**305**(5685):788-792

[3] Zheludev NI, Kivshar YS. From metamaterials to metadevices. Nature Materials. 2012;**11**(11):917-924

[4] Jahani S, Jacob Z. All-dielectric metamaterials. Nature Nanotechnology. 2016;**11**(1):23-36

[5] Yu N, Capasso F. Flat optics with designer metasurfaces. Nature Materials. 2014;**13**(2):139-150. Available from: http://www.nature.com/articles/nmat3839

[6] Arbabi E, Arbabi A, Kamali SM, Horie Y, Faraji-Dana M, Faraon A. MEMS-tunable dielectric metasurface lens. Nature Communications. 2018;**9**(1):812

[7] Lin D, Fan P, Hasman E, Brongersma ML. Dielectric gradient metasurface optical elements. Science. 2014;**345**(6194):298-302. Available from: http://www.ncbi.nlm.nih.gov/pubmed/25035488

[8] Ni X, Kildishev AV, Shalaev VM. Metasurface holograms for visible light. Nature Communications. 2013;**4**(1): 2807

[9] Zhan A, Colburn S, Trivedi R, Fryett TK, Dodson CM, Majumdar A. Low-contrast dielectric metasurface optics. ACS Photonics. 2016;**3**(2): 209-214

[10] Zheng G, Mühlenbernd H, Kenney M, Li G, Zentgraf T, Zhang S. Metasurface holograms reaching 80% efficiency. Nature Nanotechnology. 2015;**10**(4):308-312

[11] Hong C, Colburn S, Majumdar A. Flat metaform near-eye visor. Applied Optics. 2017;**56**(31):8822

[12] Yue F, Wen D, Xin J, Gerardot BD, Li J, Chen X. Vector vortex beam generation with a single plasmonic metasurface. ACS Photonics. 2016;**3**(9): 1558-1563

[13] Deng Z-L, Deng J, Zhuang X, Wang S, Li K, Wang Y, et al. Diatomic metasurface for vectorial holography. Nano Letters. 2018;**18**(5):2885-2892

[14] Zhao H, Quan B, Wang X, Gu C, Li J, Zhang Y. Demonstration of orbital angular momentum multiplexing and demultiplexing based on a metasurface in the terahertz band. ACS Photonics. 2018;**5**(5):1726-1732

[15] Semmlinger M, Zhang M, Tseng ML, Huang T-T, Yang J, Tsai DP, et al. Generating third harmonic vacuum ultraviolet light with a TiO2 metasurface. Nano Letters. 2019;**19**(12): 8972-8978

[16] Hong C, Yang S, Ndukaife JC. Optofluidic control using plasmonic TiN bowtie nanoantenna. Optical Materials Express. 2019;**9**(3):953. Available from: https://www.osapublishing.org/abstract.cfm?URI=ome-9-3-953

[17] Ndukaife JC, Kildishev AV, Agwu Nnanna AG, Wereley S, Shalaev VM, Boltasseva A. Plasmon-assisted optoelectrofluidics. In: Cleo. Washington, D.C.: OSA; 2015. p. AW3K.5

[18] Ndukaife JC, Kildishev AV, Nnanna AGA, Shalaev VM, Wereley ST, Boltasseva A. Long-range and rapid transport of individual nano-objects by a hybrid electrothermoplasmonic nanotweezer. Nature Nanotechnology. 2016;**11**(1):53-59

[19] Ndukaife JC, Mishra A, Guler U, Nnanna AGA, Wereley ST, Boltasseva A. Photothermal heating enabled by plasmonic nanostructures for electrokinetic manipulation and sorting of particles. ACS Nano. 2014; **8**(9):9035-9043

[20] Ndukaife JC, Shalaev VM, Boltasseva A. Plasmonics–turning loss into gain. Science. 2016;**351**(6271): 334-335

[21] Grier DG. A revolution in optical manipulation. Nature. Aug 2003;**424** (6950):810-816

[22] Ashkin A. Acceleration and trapping of particles by radiation pressure. Physical Review Letters. 1970;**24**(4): 156-159

[23] Ashkin A, Dziedzic JM, Bjorkholm JE, Chu S. Observation of a single-beam gradient force optical trap for dielectric particles. Optics Letters. 1986;**11**(5):288

[24] Wang K, Crozier KB. Plasmonic trapping with a gold nanopillar. ChemPhysChem. 2012;**13**(11): 2639-2648

[25] Collinge MJ, Draine BT. Discrete-dipole approximation with polarizabilities that account for both finite wavelength and target geometry. Journal of the Optical Society of America. A. 2004;**21**(10):2023

[26] Gao D, Ding W, Nieto-Vesperinas M, Ding X, Rahman M, Zhang T, et al. Optical manipulation from the microscale to the nanoscale: Fundamentals, advances and prospects. Light: Science & Applications. 2017; **6**(9):e17039-e17039

[27] Lin L, Wang M, Peng X, Lissek EN, Mao Z, Scarabelli L, et al. Opto-thermoelectric nanotweezers. Nature Photonics. 2018;**12**(4):195-201

[28] Roxworthy BJ, Johnston MT, Lee-Montiel FT, Ewoldt RH, Imoukhuede PI, Toussaint KC. Plasmonic optical trapping in biologically relevant media. PLoS One. 2014;**9**(4):e93929

[29] Crozier KB. Quo vadis, plasmonic optical tweezers? Light: Science & Applications. 3 Dec 2019;**8**(1):35

[30] Kravets VG, Kabashin AV, Barnes WL, Grigorenko AN. Plasmonic surface lattice resonances: A review of properties and applications. Chemical Reviews. 2018;**118**(12):5912-5951

[31] Juan ML, Righini M, Quidant R. Plasmon nano-optical tweezers. Nature Photonics. Jun 2011;**5**(6):349-356

[32] Shoji T, Tsuboi Y. Plasmonic optical tweezers toward molecular manipulation: Tailoring plasmonic nanostructure, light source, and resonant trapping. Journal of Physical Chemistry Letters. 2014;**5**(17):2957-2967

[33] Donner JS, Baffou G, McCloskey D, Quidant R. Plasmon-assisted optofluidics. ACS Nano. 2011;**5**(7): 5457-5462

[34] Harter T, Muehlbrandt S, Ummethala S, Schmid A, Nellen S, Hahn L, et al. Silicon–plasmonic integrated circuits for terahertz signal generation and coherent detection. Nature Photonics. 2018;**12**(10):625-633

[35] Gramotnev DK, Bozhevolnyi SI. Plasmonics beyond the diffraction limit. Nature Photonics. 2010;**4**(2):83-91

[36] Roxworthy BJ, Bhuiya AM, Inavalli VVGK, Chen H, Toussaint KC. Multifunctional plasmonic film for recording near-field optical intensity. Nano Letters. 2014;**14**(8):4687-4693

[37] Wang K, Schonbrun E, Steinvurzel P, Crozier KB. Trapping and

rotating nanoparticles using a plasmonic nano-tweezer with an integrated heat sink. Nature Communications. 2011; **2**(1):469

[38] Iacopini S, Piazza R. Thermophoresis in protein solutions. Europhysics Letters. 2003;**63**(2):247-253

[39] Duhr S, Braun D. Why molecules move along a temperature gradient. Proceedings of the National Academy of Sciences. 2006;**103**(52):19678-19682

[40] Lamhot Y, Barak A, Peleg O, Segev M. Self-trapping of optical beams through thermophoresis. Physical Review Letters. 2010;**105**(16):163906

[41] Lu GW, Gao P. Emulsions and microemulsions for topical and transdermal drug delivery. In: Handbook of Non-Invasive Drug Delivery Systems. Elsevier; 2010. pp. 59-94. Available from: https://linkinghub.elsevier.com/retrieve/pii/B9780815520252100034

[42] Derjaguin BV, Churaev NV, Muller VM. Forces near interfaces. In: Surface Forces. Boston, MA: Springer US; 1987. pp. 1-23

[43] Ramos A, Morgan H, Green NG, Castellanos A. Ac electrokinetics: A review of forces in microelectrode structures. Journal of Physics D: Applied Physics. 1998;**31**(18):2338-2353

[44] Melcher JR. Electric fields and moving media. IEEE Transactions on Education. 1974;**17**(2):100-110

[45] SQUIRES TM, BAZANT MZ. Induced-charge electro-osmosis. Journal of Fluid Mechanics. 2004;**509**: 217-252

[46] Jamshidi A, Neale SL, Yu K, Pauzauskie PJ, Schuck PJ, Valley JK, et al. NanoPen: Dynamic, low-power, and light-actuated patterning of nanoparticles. Nano Letters. 2009;**9**(8): 2921-2925

[47] Hwang H, Park J-K. Rapid and selective concentration of microparticles in an optoelectrofluidic platform. Lab on a Chip. 2009;**9**(2):199-206

[48] Elitas M, Martinez-Duarte R, Dhar N, McKinney JD, Renaud P. Dielectrophoresis-based purification of antibiotic-treated bacterial subpopulations. Lab on a Chip. 2014; **14**(11):1850-1857

[49] Zaman MA, Padhy P, Hansen PC, Hesselink L. Dielectrophoresis-assisted plasmonic trapping of dielectric nanoparticles. Physical Review A. 2017; **95**(2):023840

[50] Ndukaife JC, Xuan Y, Nnanna AGA, Kildishev AV, Shalaev VM, Wereley ST, et al. High-resolution large-ensemble nanoparticle trapping with multifunctional thermoplasmonic nanohole metasurface. ACS Nano. 2018; **12**(6):5376-5384

[51] Mittal M, Lele PP, Kaler EW, Furst EM. Polarization and interactions of colloidal particles in ac electric fields. The Journal of Chemical Physics. 2008; **129**(6):064513

[52] Work AH, Williams SJ. Characterization of 2D colloids assembled by optically-induced electrohydrodynamics. Soft Matter. 2015;**11**(21):4266-4272